

Review

High-Entropy Alloy for Thin Film Application: A Review

Nur Izzati Muhammad Nadzri ^{1,2,*}, Dewi Suriyani Che Halin ^{1,2}, Mohd Mustafa Al Bakri Abdullah ^{1,2},
Sudha Joseph ³, Mohd Arif Anuar Mohd Salleh ^{1,2}, Petrica Vizureanu ^{4,5}, Diana-Petronela Burduhos-Nergis ⁴
and Andrei Victor Sandu ^{4,6,7,*}

- ¹ Center of Excellence Geopolymer & Green Technology (CEGeoGTech), Universiti Malaysia Perlis (UniMAP), Jalan Kangar-Arau 02600, Perlis, Malaysia
 - ² Faculty of Chemical Engineering and Technology, Universiti Malaysia Perlis (UniMAP), Jalan Kangar-Arau 02600, Perlis, Malaysia
 - ³ Department of Mechanical Engineering, Cambridge Institute of Technology (CIT), Bangalore 560036, India
 - ⁴ Faculty of Materials Science and Engineering, Gheorghe Asachi Technical University of Iasi, Blvd. D. Mangeron 71, 700050 Iasi, Romania
 - ⁵ Technical Sciences Academy of Romania, Dacia Blvd 26, 030167 Bucharest, Romania
 - ⁶ Romanian Inventors Forum, Str. Sf. P. Movila 3, 700089 Iasi, Romania
 - ⁷ National Institute for Research and Development in Environmental Protection INCDPM, Splaiul Independentei 294, 060031 Bucharest, Romania
- * Correspondence: izzatinadzri@unimap.edu.my (N.I.M.N.); sav@tuiasi.ro (A.V.S.);
Tel.: +60-195516000 (N.I.M.N.)

Abstract: High entropy alloy (HEA) involves the addition of five or more elements into the materials system. This provides a multidimensional configuration space that is limitless in terms of its properties and functions. Some high-entropy alloys have already been shown to have superior properties over conventional alloys, especially the CoCr-based HEA materials. Better high-entropy alloy applications may be discovered, especially in micro- and nano-level structures, hence the development of thin film/coating -based HEA materials. Therefore, in this review paper, we are aiming to provide recent studies on the thin film/coating-based high-entropy alloy on fundamental issues related to methods of preparation, phase formation and mechanical properties. We found that sputtering has been extensively used to grow thin-film-based HEAs as it allowed parameters to be controlled with homogeneous growth. The evolution from bulk to thin samples can also be observed with the mechanical properties has exceeded the bulk-based HEA expectations, which are high hardness, better interfacial bonding and tribological behaviour and higher corrosion resistant.

Keywords: high-entropy alloy; thin films; review; high-entropy alloy thin films



Citation: Muhammad Nadzri, N.I.; Halin, D.S.C.; Al Bakri Abdullah, M.M.; Joseph, S.; Mohd Salleh, M.A.A.; Vizureanu, P.; Burduhos-Nergis, D.-P.; Sandu, A.V. High-Entropy Alloy for Thin Film Application: A Review. *Coatings* **2022**, *12*, 1842. <https://doi.org/10.3390/coatings12121842>

Academic Editor: Vincent Ji

Received: 7 November 2022

Accepted: 23 November 2022

Published: 28 November 2022

Publisher's Note: MDPI stays neutral with regard to jurisdictional claims in published maps and institutional affiliations.



Copyright: © 2022 by the authors. Licensee MDPI, Basel, Switzerland. This article is an open access article distributed under the terms and conditions of the Creative Commons Attribution (CC BY) license (<https://creativecommons.org/licenses/by/4.0/>).

1. Introduction

Most conventional alloys are based on one major metal element to form a family of alloy-based materials. However, there are limited major metal elements in the periodic table, which imposes a limitation on the development of alloy families. A new concept of alloying family was introduced by Yeh [1] and Cantor [2] that is called high-entropy alloy (HEA) where the liquid or random solid solution states have significantly higher mixing entropies than conventional alloys. Some possible mixing based on four pure elements is depicted in Figure 1. The underlying motivation stems from the simple concept that this would allow the mixture of alloys to reach a maximum configurational entropy, thus helping to stabilise the solid-solution phase against others such as the intermetallic phase. HEA is defined as an alloy containing 5 or more major elements in which the concentration of each major element should be between 5 and 35 at.%. This makes the effect of HEA more significant than conventional alloys [3–6].

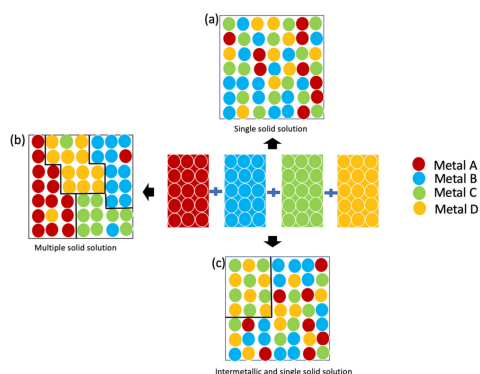


Figure 1. Possible reactions that might take place when equal amounts of four distinct elements are mixed. (a) is single solid solution, (b) is multiple solid solution and (c) is intermetallic and single solid solution.

Some of the early HEA-based materials are CrCo-based HEA, which combines with elements such as Fe, Mn, Ni and Al. Cantor [7] reported that the earlier multicomponent alloy phase (CoCrFeMnNi) with other extensive elements such as Nb and Ti and showed face-centred cubic (FCC) dendrite structures on the materials. These alloys typically favour the formation of simple and disordered solid solution structures such as face-centred cubic (FCC), body-centred cubic (BCC) and hexagonal close-packed (HCP) [8–11]. Previous works reveal that these alloys posed versatile properties such as high tensile strength and superior wear and fatigue resistance. In the past years, the focus has only been directed to the bulk materials of HEA and only limited studies are available on the development of HEA thin film-based materials [12,13]. Some of the earlier works on thin film HEA were synthesising bulk pieces of thick films using melting and other techniques such as rapid solution, thermal spray and mechanical alloying. It is also rather difficult to design suitable techniques for bulk HEA materials as they require an extremely fast cooling rate.

However, as the technology evolved, the need to find a smaller and more functional material arises, where thin film development is of interest. To date, most of the HEA-based thin films were synthesised using sputtering as it possesses advantages such as being able to control the film thickness, while stoichiometry can be adjusted by adjusting the target power and introducing a concentration gradient for one or more elements. After this review, the future research direction of HEA-based thin films will be evaluated. Therefore, it is necessary to understand a thorough literature analysis on HEA-based thin film development regarding their properties and functionality.

2. Bulk to Thin Films

Previous research on HEA focuses on bulk samples. However, as the years of miniaturisation of devices evolved, there is a need to understand this multiple alloy system at the micro to nano levels. The development of HEA research areas is as of now a hotly debated issue that can be generally partitioned into two primary classes: coatings with bulk and thin films. Some of the major issues in bulk alloy-based material is the prevalence of brittle fracture upon deformation that leads to catastrophic fracture, which typically originates from a single, major shear band. This is due to the formation of localised shear bands, which results in the lack of ductility. Chu et al. [14] conducted research on the coatings of bulk metallic glasses and discovered that the coating allows for the more uniform formation of a high density of smaller shear bands at the material interface, which in turn absorbs deformation.

Although coatings covered on bulk samples increment such as strength, certain issues still emerge, for example, the formation of different shear bands on and non-epitaxial growth of coating of bulk materials surface. Therefore, thin films are introduced because coatings on bulk materials only involve surface modification rather than microstructure

modification. To achieve maximum properties capacity, bulk samples are synthesised at the micro to nano level rather than modifying their surface.

In certain parts with multifaceted designs and surfaces, bulk structures are challenging to apply because of their high strength and hardness. However, preparing HEAs as thin films may be able to address these issues and reduce their cost, enhancing their engineering application in the future. Various deposition techniques have been explored—focusing on physical vapour deposition including laser cladding and magnetron sputtering—have been used to produce HEA coatings [8,15–17] that use little energy, making it possible to deposit thin films on substrates with complex geometry.

One of the other alternative methods is electrochemical deposition, which is a low-cost alternative to produce thin films made of alloys with a high entropy because it uses readily available raw materials and does not require complicated or expensive equipment, which can be carried out at low processing temperatures and requires controlling the thickness, morphology, while the composition of the coatings is made simple with electrodeposition by altering the deposition parameters on-aqueous solvents, and this is currently the best choice for electrodeposition of metals and alloys because of their properties high electrical conductivity, a wide working temperature range, excellent chemical and thermal stability and, most importantly, a wide electrochemical window without hydrogen evolution or hydroxide generation [15–18].

HEA thin films could also be used as diffusion barriers in future microelectronic applications due to their good thermal stability and slow diffusion [19,20]. MoNbTaW, for instance, is the subject of most of the research in thin films, just as it was in the case of bulk HEAs previously. It has a high hardness and good thermal stability [21–23]. This alloy is also a potential candidate for solid oxide fuel cell interconnects and coatings for thermoelectric elements because of its high-temperature electrical conductivity [24–27]. Because HEAs have multiple components in roughly equal atomic proportions [28], it is essential to keep the percentage of each element in the thin film nearly equal to the target during the depositing process for the precise preparation of the thin film-based HEA.

3. Thin-Film-Based High-Entropy Alloys

Due to their exceptional properties, such as high thermal stability at elevated temperatures, superior hardness and high oxidation resistance, high-entropy alloys have been primarily studied in bulk. HEA-based thin films have also recently begun to gain attention, especially in micro and nanoscale devices for use as diffusion barriers and hard coatings as these thin films produced extensive properties compared to their bulk form samples because HEA-based thin films are still able to retain their entropy stability in the micro/nano level without compromising their properties such as low Gibbs free energy which then favours a solid solution phase formation with the relatively simple crystal structure.

The quality of HEA-based thin films is affected by their growth conditions, which is equally important to obtain high-performance thin films. Among existing works on HEA thin films, the Al_x based CoCrFeNi HEA system has shown an interesting transition of structure with the Al content [29–32]. Residual stress in thin films can have a significant impact on the performance, dependability and durability of material components and devices due to their adhesion and fracture toughness of thin films. Therefore, synthesising HEA-based thin films with a suitable technique such as sputtering is very crucial.

The study by Liao et al. [33] in the earlier work on the thin film development of HEA-based materials was conducted by Dolique et al. [34], who focused on CoCr-based HEAs with a different target power (W) of deposition sputtering specifically on the FeCoNi target. Al, Cu, Fe and Ni were synthesised by magnetron sputtering technique to form mosaic targets for the AlCoCrCuFeNi thin film. AlCoCrCuFeNi were grown on Si (100) substrates with 1 μ m thickness. It was found that before annealing samples with higher power (W), the target developed polyhedron grains (100–200 nm), whereas the lower ones have spherical grains for 10–20 nm. However, during annealing, scanning electron microscopy (SEM) images revealed the presence of holes and inclusions which are caused by the silicide

formation, which was hypothesised as having been obtained from the substrate. The last step of annealing temperature (900 °C) found that only Cu and Ni remained in the thin films as other elements undergo preferential evaporation.

In an extension of previous work by Dolique et al. [34], Braeckman et al. [35] was reported on similar methods which were conducted by using powder as the sputtering target instead of a mosaic. They found that composition elements Co, Cf, Fe and Ni were varied before being cold pressed with a maximum pressure of 90 MPa. In this case, it was found that the homemade targets were not sustainable as the compositions of the films grown were not matched with the element target compositions. One of the main reasons is the high enthalpy mixing between these elements which require an extensive understanding of them. However, it was reported that the changes of phase between FCC to BCC were observed with increasing Al which is due to lattice distortion energy with regards to phase transition [36].

A more advanced technique of magnetron sputtering was conveyed by Liao et al. [33] on the CoCrFeNi with the Al_x system. Compared with previous techniques, this method uses a base pressure that is reported to be better than 1.0×10^{-6} Pa. Deposition time was varied between 15, 45, 90 to 100 min to observe the quality of the thin films. Atomic Force Microscopy (AFM) confirmed that the surface of an as-deposited thin film is homogeneous and has a smooth surface. However, it was reported that as the deposition time increased, the surface nanostructures of these thin films (missing verb) were due to the great impacts on the microstructural evolution of the thin films [37–39]. Through surface atoms diffusion and grain boundary motion, coarsening is strongly driven by the increase in deposition time [39]. The deposition time of 15 min gave a flat surface of the thin film (Figure 2a). As the system tries to reduce the surface and interface energy, the island with the lowest energy per atom will partake in the creation of a new island formation (Figure 2b,c). Therefore, when subject to deposition time for thin film growth, a continuous smooth surface will be present due to atom bombardment with the surface (Figure 2d).

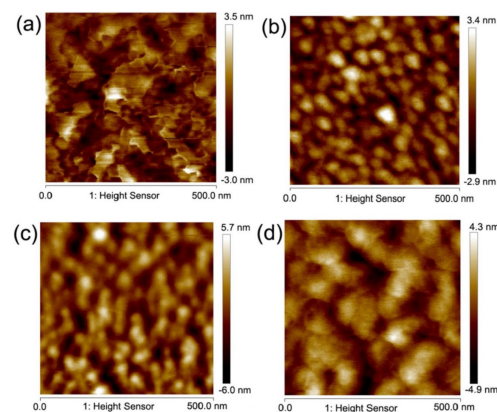


Figure 2. AFM images of $Al_{0.3}CoCrFeNi$ with different deposition times of (a) 15 min (b) 45 min (c) 90 min and (d) 180 min Reprinted with permission from Ref. [33] Copyright 2017 Elsevier.

An in-depth study of the Al-based HEA system was reported by Feng et al. [40] on the nano twins, effect subjected to mechanical properties. Different content of Al was selected to observe the changes. The synthesising technique used is similar to the one used by previous researchers which is by magnetron sputtering. The thin films were subjected to nanoindentation to observe the deformation mechanisms of submicron scales using transmission electron microscopy (TEM). It is known that the mechanical response of metals such as Cu and Ni can be significantly affected by the stability of nano twins during deformation [40]. It was reported that non-deformed areas showed a reduced volume of twinning up to 80% and significantly reduced with a lot of nano twins that were distributed throughout the columnar grains in the non-deformed area. On the other hand, in the severely deformed area, a significant number of nano twins broke down or exhibited

detwinning behaviour. The thickness of the samples was also crucial as this will determine the predominant deformation mechanism of the samples. For thicknesses less than 2 nm, the nano twins are unstable when plastic is deformed.

An et al. [41] studied a comparison of bulk and thin film CoCrCuFeNi. RF magnetron sputtering yielded thin films of CoCrCuFeNi with a thickness of 800 nm and a base pressure of 4.0×10^{-7} Pa. SEM images revealed that the as-cast CoCrCuFeNi contained a Cu-rich interdendritic phase as well as a Cu-poor dendritic phase. This is due to the mixing enthalpies and crystallization conditions between the elements. During the formation of HEA phase, a higher melting temperature initiated Cu formation ousting their boundaries (dendritic) whereas, in the liquid phase, enriched copper will crystallise at a lower temperature [42]. The interdendritic region will be present in areas with a lower percentage of Cr element because of the differences in the bulk alloys' compositions. This suggests that the current HEA alloys segregate because most of the Cr acts as a stabiliser. In contrast to the bulk alloy, which showed a strong Cu elemental separation, the CoCrCuFeNi thin films had a relatively uniform distribution of all compositions at the micromechanical scale on the surface.

It was also reported [43] that the influence of Al content in CoCrFeMn-based HEA gives larger stability of the BCC phase compared with the FCC phase, which could be due to the crystallization of CoCrMnFe-based HEA in the alpha-Mn structure. The formation of the alpha Mn phase developed highly refined columnar grains that possessed high hardness compared to other FCC-structured bulk samples [44]. This also suggests that the sputtering procedure improves the composition's uniformity. It was reported that inadequate pre-sputter led to a slight Cu enrichment in the deposited film when compared with the bulk samples in terms of the deposition technique [45,46]. During the pre-sputter process, elements with higher sputtering yield sputter faster, leaving a smaller volume fraction of these elements on the target surface.

Due to an element's total sputter rate being the production of its sputter yield and surface volume fraction, the final product of the pre-sputter process achieves a sputter rate ratio for all elements that is the same as the elemental volume fraction in the target. If the pre-sputter is insufficient, the element with a higher sputtering yield is more likely to have a sputtering rate. An inadequate pre-sputter for this alloy target will result in a higher Cu concentration in the thin film because Cu has the highest sputtering yield of all the target elements. Starting with a slightly higher Cu concentration, the CrCoCuFeNi thin film will grow at the final steady state with equal atomic ratios. Table 1 shows the summary of previous research techniques on the CoCr-based HEA thin films.

Table 1. Summary of previous studies on CoCr-based HEA coatings/thin films.

Authors	Materials	Method	Target
Dolique et al., 2010 [34]	AlCoCrCuFeNi	Magnetron sputtering	Mosaic
Zhang et al., 2011 [47]	CrCoCuFeNi	Laser cladding	Powder
An et al., 2015 [41]	CrCoCuFeNi	Magnetron sputtering	Cast metal
Braeckman et al., 2015 [35]	AlCoCrCuFeNi	Magnetron sputtering	Cast metal
Liao et al., 2017 [33]	Al0.3CoCrCuFeNi	Magnetron sputtering	Cast metal
Marshal et al., 2019 [43]	AlCoCrFeMn	Co sputtering	Alloy target
Sha et al., 2020 [44]	AlCoCrFeMn	Magnetron sputtering	Alloy target
Arfaoui et al., 2020 [48]	CrCoCuFeNi	Magnetron sputtering	Cast metal

4. Phase and Crystal Structure

The availability of properties that improve performance because of their phase and crystal structure is one of HEA's interesting aspects. Synchrotron XRD of bulk samples of CoCrCuFeNi phases revealed the presence of two FCC structure phases with slight differences in lattice constants between them. CoCrCuFeNi's thin film, on the other hand, only has one FCC structure. The film has a strong (111) FCC preferential orientation in the direction of the film's growth due to surface-energy-controlled grain growth. The

embedded atom model was used to numerically calculate the (111) family of planes, which has the lowest surface energy among materials with FCC crystalline structures.

This is because the number of unsatisfied atomic bonds decreases when planar-packing density increases. Importantly, the final film thickness has a significant impact on the degree of preferential orientation in FCC materials [38,39]. This could be because the influence of strain-energy minimisation on film thickness increases. The surface-energy factor outperforms the film strain, as demonstrated by the current experimental results. This trend may be explained by the fact that the film was deposited without an additional substrate bias at room temperature, which can significantly reduce the effect of thermal strains according to models by Carel et al. [49] and Lee [50]. The vapour deposition experiments also consistently reveal a film growth at room temperature dominated by surface energy.

This is supported by Synchrotron XRD of $\text{Al}_{0.3}\text{CoCrFeNi}$ [33] by which the thin film's fine grains are confirmed by the weak continuous rings (Figure 3a). The number of grains in the X-ray beam is limited because the thin film only has a thickness of about 2 nm. Uneven intensities in the inner ring that corresponds to the (111) plane are denoted by the red arrows. The fact that the intensity is not uniform along the rings indicates that the thin film developed a texture during sputtering. The peak positions can be indexed with the FCC structure pattern, which demonstrates that this thin film is made up of a face centre cubic phase, as shown in Figure 3b. The FCC solid solution is observed to be accompanied by a minor scattering peak. The subtle intensity of the peak suggests that the secondary phase, which was previously identified as the NiAl-type ordered BCC phase [51–53], has a low content. It is interesting to note that the main peak width also seems to be getting wider. This is mostly because the nanocrystals formed in the thin film and grew in the same direction, the preferred (111) orientation. The synchrotron radiation X-ray results show that the $\text{Al}_{0.3}\text{CoCrFeNi}$ thin film is made up of FCC solid solution nanocrystals and a small amount of NiAl-type ordered BCC phase. Additionally, the nanocrystals grow in the preferred (111) orientation.

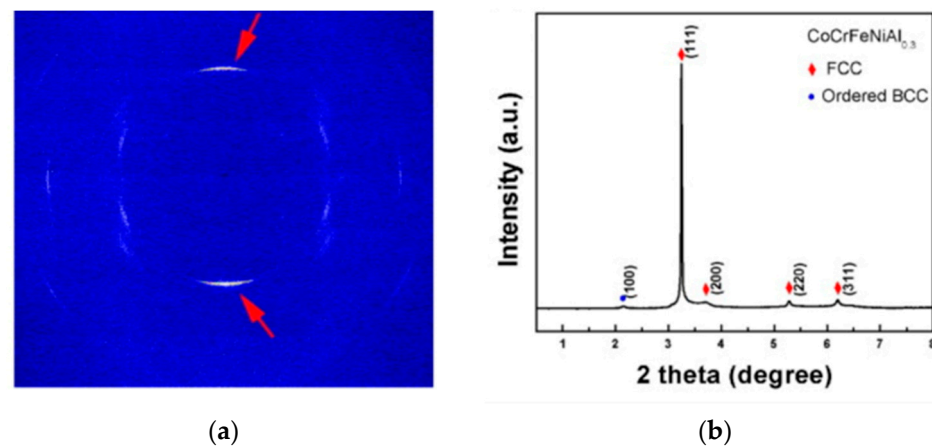


Figure 3. AFM images of $\text{Al}_{0.3}\text{CoCrFeNi}$ with different deposition times of (a) Synchrotron XRD of $\text{Al}_{0.3}\text{CoCrFeNi}$ and (b) XRD diffractogram of FCC structure for $\text{Al}_{0.3}\text{CoCrFeNi}$. Reprinted with permission from Ref. [33] Copyright 2017 Elsevier.

5. Mechanical Properties

5.1. Hardness

Nanoindentation was typically used to evaluate the thin film's mechanical properties. The indentation depth affects the film materials' hardness [12,28,54,55]; Specifically, the hardness may increase in indentation depth due to the film and substrate's distinct pile-up times and elastic modulus mismatch [41]. As a result, indentation was carried out at various depths, it measures the hardness as a function of the normalised film thickness and the indentation depth. The hardness of these thin films was usually compared to

that of various metal films described in the literature [56–58]. When compared to pure elemental metals, HEAs typically exhibit significant lattice distortion, also known as solid solution hardening due to their rigid crystal structure and strong atomic bonding, refractory metals are harder than transition metals. Thin films formed nanoscale grains during deposition, whereas traditional bulk samples typically exhibited microscale structures. The Hall–Petch relationship (i.e., grain boundary strengthening) demonstrates that grain refinement increased the hardness of crystal materials [4,6,54,59]; the applied stress required to pass dislocations across grain boundaries increased with decreasing grain size. Due to grain boundary strengthening and solid solution hardening, the thin film had a relatively high hardness.

Additionally, the degree of lattice distortion can have an impact on the mechanical properties of alloys [60]. The lattice strain in HEAs effectively retards the movement of atoms because it has been suggested that severe lattice distortion is induced in HEAs, particularly due to differences in atomic size among the alloying elements. Consequently, despite their similar elemental composition, the alloy's bulk samples and the HEA-based thin film had a superior mechanical performance. One of the reasons is because of the sputtering technique that was used from a single target prepared simply by mixing a powder blend and then sintering, we can produce high-quality thin films with uniform microstructure and high hardness.

5.2. Interfacial Bonding

Thin films are often damaged due to the structures' reliability and effectiveness of not being able to withstand buckling, film necking, cracking and delamination. As a result, a comprehensive understanding of the interfacial behaviours of thin film and substrate is essential. One of the main influences in interfacial bonding is the selection of substrates. A study conducted by Wei and Hutchinson [61] found that thick substrates will introduce delamination of prestressed (missing noun) in thin films. Plastic dissipation in either substrate or film is considered when analysing the delamination.

The growth technique is also crucial in determining the interfacial strength between HEA thin films and substrates. Non-epitaxial growth of thin film on the substrates will introduce interfacial shear stress, which leads to plastic deformation, especially at the contact edges between the film and the substrate [62,63]. Strong adhesion between film and substrate will also influence the stronger interfacial strength of the HEA-based thin films [64]. Furthermore, the competition between the effect of nanocolumn cohesion and grain size on the phase metastability in HEA-based material leads to the probability of martensitic transformation. Theoretically, for thin film-based HEA, enhanced cohesion with deposition power will prevent the formation of HCP martensite due to an increase in activation energy for martensitic transformation, whereas increased grain size with deposition power will favour the mechanical instability of the FCC parent phase because of the weakened slip obstruction. The crossover of FCC to HCP with deposition power is caused by the grain size effect dominating column cohesion at high deposition power.

HEA bulk samples usually suffer from yield strength deterioration. Efforts such as grain refinements and reduced stacking fault energy have been devoted to addressing this manner. Zhao et al. [65] studied the bonding process to CoCuFeNiTiV0.6 alloy with TiAl as the interlayer. The purpose of the interlayer is to sample stress relief. However, due to the extensively high content of pure elements, brittle samples formed at the interface between HEA and the two pure metals. Despite the extensive study on the interfacial bonding of HEA-based material, there is still no reference available on the interfacial bonding of HEA-based thin films.

5.3. Corrosion Resistant

As HEA-based materials crossed the multidisciplinary application, it is important to clarify some of the important properties such as their corrosion behaviours. CoCr-FeMnN based-HEA is reported to be pitting resistant in contrast with conventional alloys

due to having a higher passive current density compared to 316 L stainless steel and 4130 alloy [28,46,66]. Some of the important factors that affect corrosion resistance are an alloying element, method and microstructure.

Previous studies show that the enrichment region of Cu should be formed in the HEA bulk materials, which contradicts the thin film growth which was grown by magnetron sputtering that shows a lack of or no significant Cu or other element segregation. This proves that the process affects the distribution of elements in HEAs. Magnetron sputtering is a non-equilibrium process in which all kinds of atoms in the target are randomly sputtered and deposited on the substrate in a short amount of time, which is not enough for the atoms to redistribute and form a regular crystal structure with less energy [67]. In this way, the synthesis of HEA-based thin films by magnetron sputtering is exceptionally uniform at the micrometre scale. The corrosion resistance of HEA films is enhanced by the uniform distribution of these elements.

A corrosion test was conducted on CoCrFeNiAl_{0.3} thin films [68] in sodium chloride (NaCl) solution. It was found that the corrosion resistance of this HEA-based thin film is higher than 304 stainless steel because of the distributed homogeneous nanoparticles, which are relatively small and easily form a dense oxide layer that acts as a passive protective film. In addition, the elements of Co, Cr and Ni in HEA have excellent corrosion resistance, thus facilitating the build-up of the protective layer on the surface of the coating [69,70].

5.4. Tribological

When compared with the process of preparing the entire range of HEA-based material, the HEA coating/thin films can combine the common advantages of HEA alloy and the substrate. As a result, it has a greater potential for development and economic efficiency. It was reported that the addition of Mo in CoCr-based HEA coatings promoted the formation of Mo-rich BCC that led to the increase of hardness and wear resistance of the coatings [70].

Zhu et al. [69] reported on the tribological effects of Cu and Si on the materials in the CoCr-based HEA coating at two distinct temperatures. Abrasive wear caused plastic deformation in all of the samples, but as the Cu content increased, a dense oxide glaze layer that was influenced by smaller internal particle sizes and flatter interfacial bonding reduced fatigue and abrasive wear. At high temperatures, the Cu element's oxide film became denser and adheres better to the coating's surface, thus reducing wear and friction.

6. Conclusions

This review focuses on the most recent progress in HEA-based (missing noun) thin films, which was greatly influenced by their growth methods, which had an impact on the phases and crystal structure of the thin films. To gain a deeper fundamental understanding of the behaviour at the macro to nanoscale levels, comparisons between bulk and thin film samples are made. The most important aspect of synthesising a high-quality thin film material is the growth methods. Even though different elements have different sputter yields, sputtering is the most popular for depositing alloy films from a single target because the target's surface composition equilibrates after a pre-sputter step. The materials that have been sputter deposited also share similar stoichiometry as the initial target alloy. Some of the advantages of sputtering are the ability to grow homogeneous HEA-based thin films and also the ability to control the microstructure depending upon the growth parameters given, which is much more reliable than bulk sample deposition. This technique will also reduce production costs in addition to improving the materials' properties as "smaller is stronger" when it comes to thin film/coating-based materials. It will open the possibilities of producing a better and more extensive function of HEA-based thin films that will support industries such as semiconductors, hard coatings and aerospace. Future areas such as a fundamental understanding of the material structures still need to be pursued because as the number of elements increases, the mixing entropies and properties of the materials changes. This could be the key feature of determining these materials-based HEA functions and the necessary application they could play into. However, despite all the

advantages and possibilities, there is still a significant knowledge gap in this area that calls for extensive investigation.

Author Contributions: Conceptualization, N.I.M.N. and M.A.A.M.S.; introduction, D.S.C.H.; bulk to thin films, D.S.C.H. and S.J.; thin films based high-entropy alloy, M.A.A.M.S. and S.J.; mechanical properties; resources, M.M.A.B.A., N.I.M.N. and D.S.C.H.; writing—original draft preparation, D.S.C.H.; writing—review and editing, D.S.C.H., S.J., M.M.A.B.A., D.-P.B.-N. and P.V.; validation, P.V., D.-P.B.-N. and A.V.S.; funds, A.V.S. All authors have read and agreed to the published version of the manuscript.

Funding: This research received no external funding.

Institutional Review Board Statement: Not applicable.

Informed Consent Statement: Not applicable.

Data Availability Statement: The data presented in this study are available in this review.

Acknowledgments: The authors would like to acknowledge the support from the Fundamental Research Grant Scheme under grant number FRGS/1/2022/TG05/UNIMAP/02/3 from the Ministry of Education Malaysia, Center of Excellence Geopolymer & Green Technology (CEGeoGTech), Faculty of Chemical Engineering and Technology, Universiti Malaysia Perlis, (UniMAP) for their partial support. This paper was realized with the support of COMPETE 2.0 project nr.27PFE/2021, financed by the Romanian Government, Minister of Research, Innovation and Digitalization. This paper was also supported by “Gheorghe Asachi” Technical University from Iași (TUIASI), through the Project “Performance and excellence in postdoctoral research 2022”.

Conflicts of Interest: The authors declare no conflict of interest.

References

1. Yeh, J.-W. High-Entropy Alloys: Overview. In *Encyclopedia of Materials: Metals and Alloys*; Caballero, F.G., Ed.; Elsevier: Oxford, UK, 2022; pp. 294–307.
2. Senkov, O.; Rao, S.; Chaput, K.; Woodward, C. Compositional effect on microstructure and properties of NbTiZr-based complex concentrated alloys. *Acta Mater.* **2018**, *151*, 201–215. [[CrossRef](#)]
3. Miracle, D.B.; Senkov, O.N. A critical review of high entropy alloys and related concepts. *Acta Mater.* **2017**, *122*, 448–511. [[CrossRef](#)]
4. Liu, F.; Chen, S.; Wang, B.; Xiao, Y.; Wang, L.; Sun, S.; Xue, Y. High specific yield strength TiZrAlNbV high-entropy alloys via coherent nanoprecipitation strengthening. *Mater. Sci. Eng. A* **2022**, *861*, 144346. [[CrossRef](#)]
5. Murty, B.S.; Yeh, J.W.; Ranganathan, S.; Bhattacharjee, P.P. 2—High-entropy alloys: Basic concepts. In *High-Entropy Alloys*, 2nd ed.; Murty, B.S., Yeh, J.W., Ranganathan, S., Bhattacharjee, P.P., Eds.; Elsevier: Amsterdam, The Netherlands, 2019; pp. 13–30. [[CrossRef](#)]
6. Wu, P.; Liu, N.; Yang, W.; Zhu, Z.; Lu, Y.; Wang, X. Microstructure and solidification behavior of multicomponent CoCrCu_xFeMoNi high-entropy alloys. *Mater. Sci. Eng. A* **2015**, *642*, 142–149. [[CrossRef](#)]
7. Cantor, B.; Chang, I.T.H.; Knight, P.; Vincent, A.J.B. Microstructural development in equiatomic multicomponent alloys. *Mater. Sci. Eng. A* **2004**, *375–377*, 213–218. [[CrossRef](#)]
8. Senkov, O.N.; Woodward, C.F. Microstructure and properties of a refractory NbCrMo_{0.5}Ta_{0.5}TiZr alloy. *Mater. Sci. Eng. A* **2011**, *529*, 311–320. [[CrossRef](#)]
9. Murty, B.S.; Yeh, J.W.; Ranganathan, S.; Bhattacharjee, P.P. 4—Alloy design and phase selection rules in high-entropy alloys. In *High-Entropy Alloys*, 2nd ed.; Murty, B.S., Yeh, J.W., Ranganathan, S., Bhattacharjee, P.P., Eds.; Elsevier: Amsterdam, The Netherlands, 2019; pp. 51–79.
10. Li, W.; Xie, D.; Li, D.; Zhang, Y.; Gao, Y.; Liaw, P.K. Mechanical behavior of high-entropy alloys. *Prog. Mater. Sci.* **2021**, *118*, 100777. [[CrossRef](#)]
11. Yan, X.H.; Li, J.S.; Zhang, W.R.; Zhang, Y. A brief review of high-entropy films. *Mater. Chem. Phys.* **2018**, *210*, 12–19. [[CrossRef](#)]
12. Wang, A.; Ramirez, M.O.; Caplovicova, M.; Vretenar, V.; Boettcher, J.; Hopfeld, M.; Kups, T.; Flock, D.; Schaaf, P. Formation of CuCrCoFeNiO high entropy alloy thin films by rapid thermal processing of Cu/CrNiO/FeCo multilayers. *Surf. Coat. Technol.* **2020**, *405*, 126563. [[CrossRef](#)]
13. Kim, H.; Nam, S.; Roh, A.; Son, M.; Ham, M.-H.; Kim, J.-H.; Choi, H. Mechanical and electrical properties of NbMoTaW refractory high-entropy alloy thin films. *Int. J. Refract. Met. Hard Mater.* **2019**, *80*, 286–291. [[CrossRef](#)]
14. Chu, J.P.; Greene, J.; Jang, J.S.; Huang, J.; Shen, Y.-L.; Liaw, P.K.; Yokoyama, Y.; Inoue, A.; Nieh, T. Bendable bulk metallic glass: Effects of a thin, adhesive, strong, and ductile coating. *Acta Mater.* **2012**, *60*, 3226–3238. [[CrossRef](#)]

15. Soare, V.; Burada, M.; Constantin, I.; Mitrică, D.; Bădiliță, V.; Caragea, A.; Târcolea, M. Electrochemical deposition and microstructural characterization of AlCrFeMnNi and AlCrCuFeMnNi high entropy alloy thin films. *Appl. Surf. Sci.* **2015**, *358*, 533–539. [[CrossRef](#)]
16. Wang, S.; Guo, X.; Yang, H.; Dai, J.; Zhu, R.; Gong, J.; Peng, L.; Ding, W. Electrodeposition mechanism and characterization of Ni–Cu alloy coatings from a eutectic-based ionic liquid. *Appl. Surf. Sci.* **2014**, *288*, 530–536. [[CrossRef](#)]
17. Simka, W.; Puszczczyk, D.; Nawrat, G. Electrodeposition of metals from non-aqueous solutions. *Electrochim. Acta* **2009**, *54*, 5307–5319. [[CrossRef](#)]
18. Pavithra, C.L.P.; Janardhana, R.K.S.K.; Reddy, K.M.; Murapaka, C.; Joardar, J.; Sarada, B.V.; Tamboli, R.R.; Hu, Y.; Zhang, Y.; Wang, X.; et al. An advancement in the synthesis of unique soft magnetic CoCuFeNiZn high entropy alloy thin films. *Sci. Rep.* **2021**, *11*, 8836. [[CrossRef](#)] [[PubMed](#)]
19. Kozak, R.; Steurer, W. High-entropy alloys. *Acta Crystallogr. Sect. A Found. Crystallogr.* **2013**, *69*, s497. [[CrossRef](#)]
20. Tsai, M.-H. Physical Properties of High Entropy Alloys. *Entropy* **2013**, *15*, 5338–5345. [[CrossRef](#)]
21. Quammen, R.N.; Rottmann, P.F. Investigation of low temperature oxidation behavior of MoNbTaW thin films. *J. Alloys Compd.* **2022**, *900*, 163373. [[CrossRef](#)]
22. Han, J.; Su, B.; Lu, J.; Meng, J.; Zhang, A.; Wu, Y. Preparation of MoNbTaW refractory high entropy alloy powders by pressureless spark plasma sintering: Crystal structure and phase evolution. *Intermetallics* **2020**, *123*, 106382. [[CrossRef](#)]
23. Gruber, G.C.; Lassnig, A.; Zak, S.; Gammer, C.; Cordill, M.J.; Franz, R. Synthesis and structure of refractory high entropy alloy thin films based on the MoNbTaW system. *Surf. Coat. Technol.* **2022**, *439*, 128446. [[CrossRef](#)]
24. Li, Z.; Tian, Y.; Teng, C.; Cao, H. Recent Advances in Barrier Layer of Cu Interconnects. *Materials* **2020**, *13*, 5049. [[CrossRef](#)] [[PubMed](#)]
25. Xia, A.; Dedoncker, R.; Glushko, O.; Cordill, M.J.; Depla, D.; Franz, R. Influence of the nitrogen content on the structure and properties of MoNbTaVW high entropy alloy thin films. *J. Alloys Compd.* **2020**, *850*, 156740. [[CrossRef](#)]
26. Smeltzer, J.A.; Hornbuckle, B.C.; Giri, A.K.; Darling, K.A.; Harmer, M.P.; Chan, H.M.; Marvel, C.J. Nitrogen-induced hardening of refractory high entropy alloys containing laminar ordered phases. *Acta Mater.* **2021**, *211*, 116884. [[CrossRef](#)]
27. Dąbrowa, J.; Kucza, W.; Cieślak, G.; Kulik, T.; Danielewski, M.; Yeh, J.-W. Interdiffusion in the FCC-structured Al-Co-Cr-Fe-Ni high entropy alloys: Experimental studies and numerical simulations. *J. Alloys Compd.* **2016**, *674*, 455–462. [[CrossRef](#)]
28. Lu, T.-W.; Feng, C.-S.; Wang, Z.; Liao, K.-W.; Liu, Z.-Y.; Xie, Y.-Z.; Hu, J.-G.; Liao, W.-B. Microstructures and mechanical properties of CoCrFeNiAl_{0.3} high-entropy alloy thin films by pulsed laser deposition. *Appl. Surf. Sci.* **2019**, *494*, 72–79. [[CrossRef](#)]
29. Wu, Z.; Wang, X.; Cao, Q.; Zhao, G.; Li, J.; Zhang, D.; Zhu, J.-J.; Jiang, J. Microstructure characterization of Al_xCo₁Cr₁Cu₁Fe₁Ni₁ (x = 0 and 2.5) high-entropy alloy films. *J. Alloys Compd.* **2014**, *609*, 137–142. [[CrossRef](#)]
30. Sharma, A.; Oh, M.C.; Ahn, B. Microstructural evolution and mechanical properties of non-Cantor AlCuSiZnFe lightweight high entropy alloy processed by advanced powder metallurgy. *Mater. Sci. Eng. A* **2020**, *797*, 140066. [[CrossRef](#)]
31. Ng, C.; Guo, S.; Luan, J.; Wang, Q.; Lu, J.; Shi, S.-Q.; Liu, C.T. Phase stability and tensile properties of Co-free Al_{0.5}CrCuFeNi₂ high-entropy alloys. *J. Alloys Compd.* **2014**, *584*, 530–537. [[CrossRef](#)]
32. WChang, S.-Y.; Lin, S.-Y.; Huang, Y.-C. Microstructures and mechanical properties of multi-component (AlCrTaTiZr)_{N_x}C_y nanocomposite coatings. *Thin Solid Films* **2011**, *519*, 4865–4869. [[CrossRef](#)]
33. Liao, W.; Lan, S.; Gao, L.; Zhang, H.; Xu, S.; Song, J.; Wang, X.; Lu, Y. Nanocrystalline high-entropy alloy (CoCrFeNiAl_{0.3}) thin-film coating by magnetron sputtering. *Thin Solid Films* **2017**, *638*, 383–388. [[CrossRef](#)]
34. Dolique, V.; Thomann, A.-L.; Brault, P.; Tessier, Y.; Gillon, P. Thermal stability of AlCoCrCuFeNi high entropy alloy thin films studied by in-situ XRD analysis. *Surf. Coat. Technol.* **2010**, *204*, 1989–1992. [[CrossRef](#)]
35. Braeckman, B.; Boydens, F.; Hidalgo, H.; Dutheil, P.; Jullien, M.; Thomann, A.-L.; Depla, D. High entropy alloy thin films deposited by magnetron sputtering of powder targets. *Thin Solid Films* **2015**, *580*, 71–76. [[CrossRef](#)]
36. Braeckman, B.; Depla, D. Structure formation and properties of sputter deposited Nb_x-CoCrCuFeNi high entropy alloy thin films. *J. Alloys Compd.* **2015**, *646*, 810–815. [[CrossRef](#)]
37. Xie, L.; Brault, P.; Thomann, A.-L.; Bauchire, J.-M. AlCoCrCuFeNi high entropy alloy cluster growth and annealing on silicon: A classical molecular dynamics simulation study. *Appl. Surf. Sci.* **2013**, *285*, 810–816. [[CrossRef](#)]
38. Thornton, J.A.; Hoffman, D. Stress-related effects in thin films. *Thin Solid Films* **1989**, *171*, 5–31. [[CrossRef](#)]
39. Mahieu, S.; Ghekiere, P.; Depla, D.; De Gryse, R. Biaxial alignment in sputter deposited thin films. *Thin Solid Films* **2006**, *515*, 1229–1249. [[CrossRef](#)]
40. Feng, X.; Fu, W.; Zhang, J.; Zhao, J.; Li, J.; Wu, K.; Liu, G.; Sun, J. Effects of nanotwins on the mechanical properties of Al_xCoCrFeNi high entropy alloy thin films. *Scr. Mater.* **2017**, *139*, 71–76. [[CrossRef](#)]
41. An, Z.; Jia, H.; Wu, Y.; Rack, P.D.; Patchen, A.D.; Liu, Y.; Ren, Y.; Li, N.; Liaw, P.K. Solid-Solution CrCoCuFeNi High-Entropy Alloy Thin Films Synthesized by Sputter Deposition. *Mater. Res. Lett.* **2015**, *3*, 203–209. [[CrossRef](#)]
42. Ustinov, A.; Demchenkov, S.; Melnychenko, T.; Skorodzievskii, V.; Polishchuk, S. Effect of structure of high entropy CrFeCoNiCu alloys produced by EB PVD on their strength and dissipative properties. *J. Alloys Compd.* **2021**, *887*, 161408. [[CrossRef](#)]
43. Marshal, A.; Pradeep, K.G.; Music, D.; Wang, L.; Petravic, O.; Schneider, J. Combinatorial evaluation of phase formation and magnetic properties of FeMnCoCrAl high entropy alloy thin film library. *Sci. Rep.* **2019**, *9*, 7864. [[CrossRef](#)]
44. Sha, C.; Zhou, Z.; Xie, Z.; Munroe, P. Extremely hard, α-Mn type high entropy alloy coatings. *Scr. Mater.* **2020**, *178*, 477–482. [[CrossRef](#)]

45. Butler, T.M.; Alfano, J.P.; Martens, R.L.; Weaver, M.L. High-Temperature Oxidation Behavior of Al-Co-Cr-Ni-(Fe or Si) Multicomponent High-Entropy Alloys. *Jom* **2014**, *67*, 246–259. [[CrossRef](#)]
46. Zhang, H.; Pan, Y.; He, Y.-Z. Synthesis and characterization of FeCoNiCrCu high-entropy alloy coating by laser cladding. *Mater. Des.* **2011**, *32*, 1910–1915. [[CrossRef](#)]
47. Arfaoui, M.; Radnóczy, G.; Kis, V.K. Transformations in CrFeCoNiCu High Entropy Alloy Thin Films during In-Situ Annealing in TEM. *Coatings* **2020**, *10*, 60. [[CrossRef](#)]
48. Carel, R.; Thompson, C.; Frost, H. Computer simulation of strain energy effects vs surface and interface energy effects on grain growth in thin films. *Acta Mater.* **1996**, *44*, 2479–2494. [[CrossRef](#)]
49. Lee, D.N. A model for development of orientation of vapour deposits. *J. Mater. Sci.* **1989**, *24*, 4375–4378. [[CrossRef](#)]
50. Choudhuri, D.; Gwalani, B.; Gorsse, S.; Mikler, C.; Ramanujan, R.; Gibson, M.; Banerjee, R. Change in the primary solidification phase from fcc to bcc-based B2 in high entropy or complex concentrated alloys. *Scr. Mater.* **2017**, *127*, 186–190. [[CrossRef](#)]
51. Guo, S.; Ng, C.; Lu, J.; Liu, C.T. Effect of valence electron concentration on stability of fcc or bcc phase in high entropy alloys. *J. Appl. Phys.* **2011**, *109*, 103505. [[CrossRef](#)]
52. Guo, S.; Hu, Q.; Ng, C.; Liu, C. More than entropy in high-entropy alloys: Forming solid solutions or amorphous phase. *Intermetallics* **2013**, *41*, 96–103. [[CrossRef](#)]
53. Wang, C.; Li, T.-H.; Liao, Y.-C.; Li, C.-L.; Jang, J.S.-C.; Hsueh, C.-H. Hardness and strength enhancements of CoCrFeMnNi high-entropy alloy with Nd doping. *Mater. Sci. Eng. A* **2019**, *764*. [[CrossRef](#)]
54. Zhou, Q.; Du, Y.; Han, W.; Jia, Q.; Deng, Y.; Wang, H. Identifying the high entropy effect on plastic dynamics in bulk metallic glasses: A nanoindentation study at room and elevated temperatures. *Mater. Des.* **2020**, *189*, 108500. [[CrossRef](#)]
55. Kumar, K.; Van Swygenhoven, H.; Suresh, S. Mechanical behavior of nanocrystalline metals and alloys. *Acta Mater.* **2003**, *51*, 5743–5774. [[CrossRef](#)]
56. Dubey, D.k.; Yadav, R.A.K.; Lee, M.; Khan, S.; Liang, T.-W.; Jou, J.-H. Effect of molecular energy level of electron transport layer on recombination zone in OLED. In Proceedings of the 2018 25th International Workshop on Active-Matrix Flatpanel Displays and Devices (AM-FPD), Kyoto, Japan, 3–6 July 2018; pp. 1–3. [[CrossRef](#)]
57. Gludovatz, B.; George, E.P.; Ritchie, R.O. Processing, Microstructure and Mechanical Properties of the CrMnFeCoNi High-Entropy Alloy. *JOM* **2015**, *67*, 2262–2270. [[CrossRef](#)]
58. Kang, B.; Lee, J.; Ryu, H.J.; Hong, S.H. Ultra-high strength WNbMoTaV high-entropy alloys with fine grain structure fabricated by powder metallurgical process. *Mater. Sci. Eng. A* **2018**, *712*, 616–624. [[CrossRef](#)]
59. Wei, Y.; Hutchinson, J.W. Nonlinear delamination mechanics for thin films. *J. Mech. Phys. Solids* **1997**, *45*, 1137–1159. [[CrossRef](#)]
60. Guo, W.; Chen, P.; Liu, H.; Peng, G.; Zhu, J.; Wu, Y. Interfacial behavior of thin film bonded to plastically graded substrate under tensile loading. *Eur. J. Mech.—A/Solids* **2023**, *97*, 104818. [[CrossRef](#)]
61. Lee, C.; Song, G.; Gao, M.C.; Feng, R.; Chen, P.; Brechtel, J.; Chen, Y.; An, K.; Guo, W.; Poplawsky, J.D.; et al. Lattice distortion in a strong and ductile refractory high-entropy alloy. *Acta Mater.* **2018**, *160*, 158–172. [[CrossRef](#)]
62. Jiang, M.; Xu, K.; Liao, N.; Zheng, B. Effect of sputtering power on piezoresistivity and interfacial strength of SiCN thin films prepared by magnetic sputtering. *Ceram. Int.* **2022**, *48*, 2112–2117. [[CrossRef](#)]
63. Zhao, G.; Zhang, J.; Zhang, S.; Wang, G.; Han, J.; Zhang, C. Interfacial microstructure and mechanical properties of TiAl alloy/TC4 titanium alloy joints diffusion bonded with CoCuFeNiTiV_{0.6} high entropy alloy interlayer. *J. Alloys Compd.* **2023**, *935*, 167987. [[CrossRef](#)]
64. Muftah, W.; Allport, J.; Vishnyakov, V. Corrosion performance and mechanical properties of FeCrSiNb amorphous equiatomic HEA thin film. *Surf. Coat. Technol.* **2021**, *422*, 127486. [[CrossRef](#)]
65. Huang, K.; Zhou, X.; Guo, H.; Chen, Y. Thermal annealing effect on the corrosion resistance of AlCuNiTiZr high entropy alloy films in sulfuric acid solution. *Thin Solid Films* **2021**, *730*, 138707. [[CrossRef](#)]
66. Guo, Y.; Liu, L.; Zhang, W.; Yao, K.; Zhao, Z.; Shang, J.; Qi, J.; Chen, M.; Zhao, R.; Wu, F. Effects of electromagnetic pulse treatment on spinodal decomposed microstructure, mechanical and corrosion properties of AlCoCrFeNi high entropy alloy. *J. Alloys Compd.* **2021**, *889*, 161676. [[CrossRef](#)]
67. Mohamed, O.; Hassan, M.; Egilmez, M.; Abuzaid, W.; Ibrahim, T.; Khamis, M. Corrosion behavior of CoCrNi/mild steel medium entropy alloy thin films. *Mater. Today Commun.* **2021**, *30*, 103015. [[CrossRef](#)]
68. Lv, Y.; Lang, X.; Zhang, Q.; Liu, W.; Liu, Y. Study on corrosion behavior of (CuZnMnNi)_{100-x}Sn_x high-entropy brass alloy in 5 wt% NaCl solution. *J. Alloys Compd.* **2022**, *921*, 166051. [[CrossRef](#)]
69. Zhu, Z.-X.; Liu, X.-B.; Liu, Y.-F.; Zhang, S.-Y.; Meng, Y.; Zhou, H.-B. Effects of Cu/Si on the microstructure and tribological properties of FeCoCrNi high entropy alloy coating by laser cladding. *Wear* **2023**, *512–513*, 204533. [[CrossRef](#)]
70. Sha, M.; Jia, C.; Qiao, J.; Feng, W.; Ai, X.; Jing, Y.-A.; Shen, M.; Li, S. Microstructure and Properties of High-Entropy Al_xCoCrFe_{2.7}MoNi Alloy Coatings Prepared by Laser Cladding. *Metals* **2019**, *9*, 1243. [[CrossRef](#)]